A Carboniferous apex for the late Paleozoic icehouse

N. Griffis[1]*, R. Mundil[2], I. Montañez[3], D. Le Heron[4], P. Dietrich[5] and R. Iannuzzi[6]

[1]US Geological Survey, Geology Geochemistry and Geophysics Science Center, Lakewood, CO 80225, USA

[2]Berkeley Geochronology Center, 2455 Ridge Rd, Berkeley, CA, 94709, USA

[3]University of California, Davis, One Shields Ave, Davis, CA, 95618, USA

[4]Department of Geodynamics and Sedimentology, University of Vienna, Althanstrasse 14, A-1090 Vienna, Austria

[5]Géosciences-Rennes, UMR6118, Université de Rennes 1, 35042 Rennes Cedex, France

[6]Departamento de Paleontologia e Estratigrafia, Universidade Federal Rio Grande do Sul, Porto Alegre, Rio Grande do Sul 90040-060, Brazil

NG, 0000-0002-2506-7549
*Correspondence: ngriffis@usgs.gov

Abstract: Icehouse climate systems occur across an abbreviated portion of Earth history, constituting *c.* 25% of the Phanerozoic record. The Late Paleozoic Ice Age (LPIA) was the most extreme and longest lasting glaciation of the Phanerozoic and is characterized by periods of acute continental-scale glaciation, separated by periods of ice minima or ice-free conditions on the order of $<10^6$ years. The late Paleozoic glaciogenic record of the Paraná and Kalahari basins of southern Gondwana form one of the largest, best-preserved and well-calibrated records of this glaciation. In the Carboniferous, the eastern and southern margins of the Paraná Basin and the Kalahari Basin were characterized by subglacial conditions, with evidence for continental and upland glaciers. In the latest Carboniferous, these basins transitioned from subglacial reservoirs to ice-free or 'ice distal' conditions evidenced by the widespread deposition of marine deposits juxtaposed on subglacial bedforms. High-precision U–Pb zircon chemical abrasion thermal ionization mass spectrometry geochronological constraints from volcanic ash deposits in the deglacial marine black shales of the Kalahari Basin and from fluvial and coal successions, which overlie marine deposits in the Paraná Basin, indicate subglacial evidence in these regions is constrained to the Carboniferous. The loss of ice in these regions is congruent with a late Carboniferous peak in pCO_2 and widespread marine anoxia in the late Carboniferous. The permeant retreat of glaciers in basinal settings, despite an early Permian pCO_2 nadir, highlights the influence of short-term perturbations on the longer-term CO_2 record and suggests an ice threshold had been crossed in the latest Carboniferous. A definitive driver for greenhouse gases in the LPIA, such as abundant and sustained volcanic activity or an increased biological pump driven by ocean fertilization, is unresolved for this period. Lastly, the proposed Carboniferous apex for the high-latitude LPIA record is incongruent with observations from the low-latitude tropics where an early Permian peak is proposed.

The Late Paleozoic Ice Age (LPIA) was the most severe and longest lasting glaciation of the Phanerozoic and the only example of an icehouse–greenhouse turnover in a world colonized by complex terrestrial life (Gastaldo *et al.* 1996; Montañez and Poulsen 2013). Interpretation of the nature, scale and dynamics of the late Paleozoic ice record has evolved from a single massive ice sheet centred over polar Gondwana, which lasted for the extent of the *c.* 60 myr icehouse, to a more dynamic record, one characterized by multiple continental and alpine ice centres with phases of intense glaciation, separated by shorter intervals of diminished ice (Fielding *et al.* 2008; Isbell *et al.* 2008; Montañez 2022). The LPIA glacial record is interpreted as diachronous, with deglaciation occurring first in alpine regions of SW Gondwana by the late Visean, whereas large ice masses lasted at least into the late early Permian in polar Gondwana (Gulbranson *et al.* 2010; Isbell *et al.* 2012; Griffis *et al.* 2019*a*, *b*, 2021). A diachronous ice record highlights the importance of long-term (10^6 to 10^8 years) tectonic constraints (i.e. topography and latitude) on Gondwanan ice distribution (Isbell *et al.* 2012; Griffis *et al.* 2019*a*, *b*). An exportable chronostratigraphic framework based on high-resolution U–Pb zircon geochronology, developed over recent years for southern Gondwana, provides radioisotopic age constraints on the ice record and reveals the presence of isochronous deglaciation events that can be correlated at the $<10^6$-year timescale, and are *c.* 1–2 myr in duration. The presence of widespread, short-lived deglaciation events suggests a shorter duration, climate-forcing driver of late Paleozoic climatic amelioration (Griffis *et al.* 2019*a*).

From: Lucas, S. G., DiMichele, W. A., Opluštil, S. and Wang, X. (eds) *Ice Ages, Climate Dynamics and Biotic Events: the Late Pennsylvanian World*. Geological Society, London, Special Publications, **535**,
https://doi.org/10.1144/SP535-2022-256

At least three major isochronous deglaciation events are documented across southern and southwestern Gondwana, occurring at *c.* 300–299 Ma, 296 Ma and 282 Ma (Griffis *et al.* 2019*a*). Deglaciation events correspond with increased pCO_2, highlighting the influence of climatic forcing on the Gondwanan glacial record (Griffis *et al.* 2019*a*, 2021). The latest Carboniferous event (300–299 Ma) was one of the most acute and associated with unrecoverable ice across large regions of Gondwana and suggests a Carboniferous apex for the LPIA (Chen *et al.* 2016; Griffis *et al.* 2019*a*, *b*, 2021; Chen *et al.* 2022).

The late Carboniferous was a period of pronounced climatic change associated with periods of near doubling of pCO_2 from mid Carboniferous lows, the repeated turnover of plant communities across the Euramerican tropics, ocean anoxia accompanied by widespread deposition of black shales in marine depositional basins and the loss of glaciogenic deposits across much of southern Gondwana (Cleal and Thomas 2005; Montañez and Poulsen 2013; Montañez *et al.* 2016; Richey *et al.* 2020; Chen *et al.* 2022). Southern Gondwanan depositional basins record a rich archive of the response to late Paleozoic climatic forcing, with many basins transitioning from ice-proximal and subglacial to ice-free or ice-distal reservoirs by the late Carboniferous. In particular, the mid- to high-latitude Paraná and Kalahari basins of Brazil and Namibia, respectively, host arguably the world's highest fidelity record of this transition given the abundance of core and outcrop data across these passive intracratonic basins, the well-preserved nature of the glacial record and the large area over which glaciogenic deposits can be traced. Sedimentological studies and detrital zircon geochronology have documented one of the richest Phanerozoic archives of the dynamic nature of late Paleozoic glaciation in this region, documenting a glaciogenic record characterized by multiple advance–retreat cycles before transitioning into postglacial marine or littoral depositional systems (Vesely *et al.* 2015, 2018; Mottin *et al.* 2018; Fedorchuk *et al.* 2019*a*, *b*; Griffis *et al.* 2019*b*; Zieger *et al.* 2019; Dietrich *et al.* 2021; Le Heron *et al.* 2021). Furthermore, high-resolution U–Pb zircon chemical abrasion thermal ionization mass spectrometry (CA-TIMS) calibrated ages for these successions allows for the establishment of a multi-basin stratigraphic framework across this region, which can be used to investigate the nature of the mid to late Carboniferous glaciogenic system.

In this contribution, we briefly review the late Carboniferous and earliest Permian sedimentological and stratigraphic histories of the Paraná and Kalahari basins with a particular focus on the nature of the glaciation across this region and the ensuing climatic transition. We show that the Carboniferous was an apex of ice extent for the late Paleozoic icehouse across much of southern Gondwana, which was succeeded by an abrupt late Carboniferous warming. We explore some of the possible drivers for ice loss, which are still unresolved. Furthermore, our observations of unrecoverable high-latitude ice in the latest Carboniferous presents a paradox, where high-latitude ice sheets are collapsing at a time when high elevation areas in the low latitudes are proposed to have experienced glacial conditions (Soreghan *et al.* 2008, 2014, 2019; Pfeifer *et al.* 2021). Additionally, we briefly review the glaciogenic record from Gondwana and the temporal constraints for these deposits.

Nature and temporal constraints of SW Gondwana late Paleozoic glacial record

Upper Paleozoic glaciogenic rocks are found on all continents that compose the supercontinent of Gondwana (Isbell *et al.* 2003; Milani and De Witt 2008; Linol *et al.* 2016; López-Gamundí *et al.* 2021; Montañez 2022). The stratigraphic histories of the intracratonic Paraná and Kalahari basins form one of the highest fidelity records of the LPIA and the ultimate turnover to greenhouse climate conditions by the late early Permian. The Paraná and Kalahari basins cover an area of *c.* 3×10^6 km^2, spanning the mid- to high latitudes of southwestern and southern Gondwana (*c.* 50° S Paraná; 65° S Kalahari; Fig. 1; Griffis *et al.* 2021). Importantly, these intracratonic basins experienced minimal tectonic influence, with flat-lying glaciogenic rocks traced laterally over large areas in outcrop or through cores that are often capped by Mesozoic flood basalts, preserving one of the best sedimentological archives of the LPIA (Milani and De Witt 2008; Dietrich *et al.* 2021). In outcrop, the stratigraphic arrangement of facies across this region is largely similar, with all basins typically hosting a major subglacial unconformity along the basin margins, occurring between Precambrian–Cambrian or Devonian basement, and which is typically overlain by either glacial marine, glacial lacustrine or continental glaciogenic deposits (González-Bonorino and Eyles 1995). The glaciogenic system often records multiple ice advance–retreat cycles, which manifest as subglacial or ice proximal facies that are overlain by deeper water depositional facies and eventually capped by fluvial/deltaic successions (Visser 1983, 1997; Holz *et al.* 2010; Fallgatter and Paim 2019; Griffis *et al.* 2019*a*, *b*, 2021). Here, we briefly discuss the nature and dynamics of the southern Gondwana glaciogenic record, with a particular focus on an acute late Carboniferous deglaciation and the immediate postglacial successions of southern Brazil

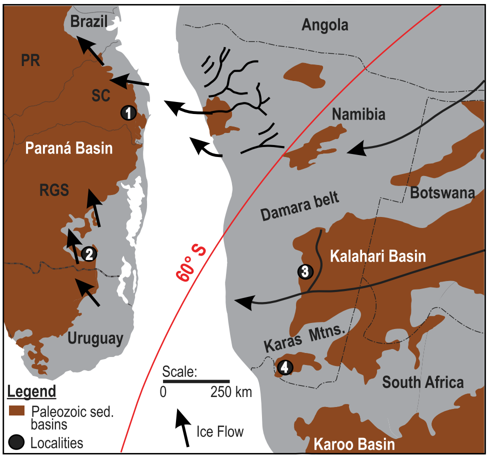

Fig. 1. Palaeogeographic map of the late Paleozoic of SW Gondwana (300 Ma). Sedimentary basins (brown) overlain on present-day Brazil and Uruguay in SE South America and Namibia, South Africa, Botswana and Angola in SW Africa. Black arrows indicate ice flow directions across Namibia and Brazil (Visser 1987; Gesicki *et al.* 2002; Rosa *et al.* 2016; Assine *et al.* 2018). Localities: 1 – Anitápolis (from drill core section), Santa Catarina State; 2 – Candiota (from drill core section), Rio Grande do Sul State; 3 – Tses (from outcrop section), Namibia, Aranos sub-basin; 4 – Zwartbas (from outcrop section), Namibia, Karasburg sub-basin. PR, Paraná State; SC, Santa Catarina State; RGS, Rio Grande do Sul State.

and Namibia. The Paraná and Kalahari basins have been the targets for multiple geochronological studies focused on refining the age control for the late Paleozoic succession and Gondwanan glaciations (cf. Bangert *et al.* 1999; Stollhofen *et al.* 2008; Cagliari *et al.* 2016). An extensive review of the previous studies can be found in Griffis *et al.* (2018, 2019*a*, 2021). In this contribution we concentrate on areas where U–Pb zircon CA-TIMS ages are reported, which is considered one of the most accurate and precise geochronological methods and enables the establishment of a regional stratigraphic framework to test the synchroneity and timing of ice loss across these basins.

Paraná Basin

The Paraná Basin is one of the largest depocentres of upper Paleozoic rocks in South America (Fig. 1), where glaciogenic deposits cover an area of 1×10^6 km^2 and reach up to 1.3 km in thickness in subsurface cores (Eyles *et al.* 1993; Rocha-Campos *et al.* 2008). The glaciogenic rocks are constrained to the Itararé Group, which records anywhere from one to five glacial–interglacial cycles across the Lagoa Azul through Taciba formations (Vesely *et al.* 2015; Griffis *et al.* 2019*b*). In this contribution we focus solely on the records from Rio Grande do Sul and Santa Catarina states, where the glaciogenic facies attain a thickness of from tens (Rio Grande do Sul State, southern Paraná Basin) to hundreds of metres (Santa Catarina State, southeastern Paraná Basin; Fig. 2). In these southern regions the glaciogenic record is highly dynamic, recording multiple ice advance–retreat cycles, interpreted to represent glacial continental and glacial marine facies, with the thickest and most continuous deposits occurring across the southeastern Paraná Basin within Santa Catarina State. Thick fluvial, estuarine and coal deposits cap the glaciogenic systems and host U–Pb zircon dated volcanic ash horizons, which provide age constraints for the final demise of ice in this region. Here we briefly review the glaciogenic and immediate postglacial record from Rio Grande do Sul and Santa Catarina states and the established chronostratigraphic framework for the region.

Subglacial erosional features, which include scoured palaeovalleys, roche moutonnée, striated pavements and larger streamlined bedrock features, record the initial advance of glaciers across the southern Paraná Basin (Figs 2 & 3a; Gesicki *et al.* 2002; Rocha-Campos *et al.* 2008; Assine *et al.* 2018). In Rio Grande do Sul State, push moraine complexes that record multiple advance–retreat cycles, striated pavements and soft-sediment deformed glacial plough structures indicate the presence of dynamic grounded glaciers across southern Brazil (Figs 2 & 3a; Tomazelli and Soliani Júnior 1997; Fedorchuk *et al.* 2019*b*). In Uruguay, *c.* 100 km to the south of Rio Grande do Sul State, asymmetrical streamlined landforms, interpreted as whale backs, which formed by the erosion of an overriding glacier, confirm the presence of grounded ice in this region (Assine *et al.* 2018). In Santa Cataria State (SE Paraná Basin), palaeovalleys up to 500 m wide and 40 m deep were carved into Precambrian basement along the eastern margin of the basin, recording the initial ice advance. Linear striations, as well as gouged and polished surfaces, which are found within and along the margins of the palaeovalleys, attest to subglacial erosion. The palaeovalley infill records multiple ice advance–retreat cycles, composed of marine black shales, rhythmites, mass transport and dropstone-poor diamictites, indicating a dynamic glaciation (Figs 2 & 3c; Fallgatter and Paim 2019). Palaeoflow indicators across the south and SE margin of the Paraná Basin suggests an overall north to NW flow of ice into the basin, with ice emanating from at least two distinct African ice centres (Fig. 1; Gesicki *et al.* 2002; Rosa *et al.* 2016; Assine *et al.* 2018; Griffis *et al.* 2019*b*, 2021; Fedorchuk *et al.* 2021). Detrital zircon geochronology from across the south and SE margin of the

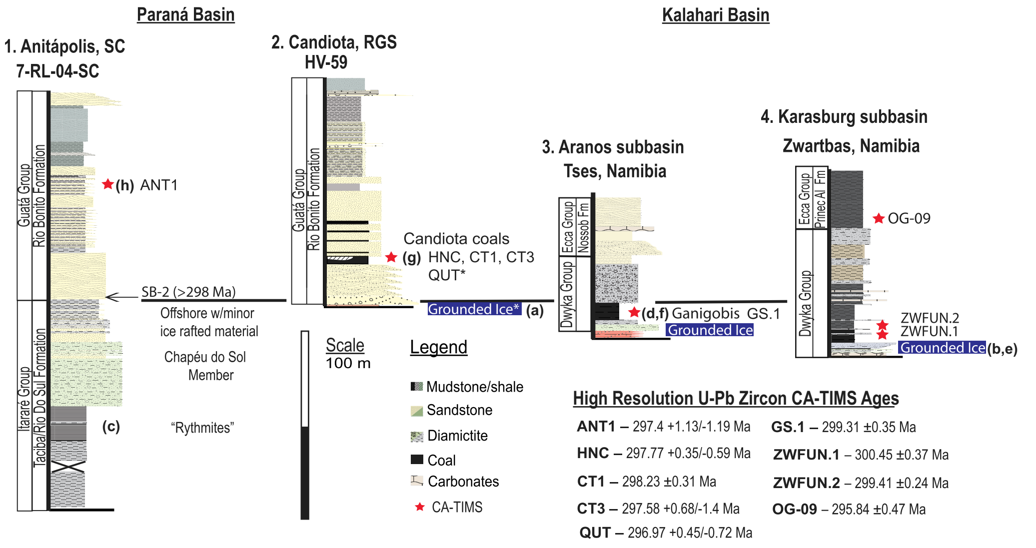

Fig. 2. Stratigraphic framework of the upper Carboniferous–lower Permian for the Paraná and Kalahari basins. Header number above the stratigraphic section refers to map locations in Figure 1. SB-2 (sequence-boundary 2) from Holz *et al.* (2008) in the Anitápolis section is defined by the juxtaposition of fluvial sandstones on top of marine rocks (>298 Ma). The Taciba Formation is the uppermost unit of the Itararé Group, though in the regions of Santa Catarina and Rio Do Sul states, the upper Itararé is referred to as the Rio Do Sul Formation (Holz *et al.* 2010). Correlations into the Kalahari Basin are built based on U–Pb CA-TIMS ages (red stars). All evidence for grounded ice occurs below SB-2 in the Paraná Basin and below the Ganigobis Shale Member and correlative shales in the Zwartbas region in the Kalahari Basin. Letters refer to stratigraphic location of images in Figure 3. Reported CA-TIMS ages from Griffis *et al.* (2018, 2019*a*, 2021). * Denotes approximate locations for Quitéria ash (QUT) and striated surface, which are projected into the Candiota section (Griffis *et al.* 2019*a*). Red samples: ANT1, Anitápolis 1; HNC, Hulha Negra Candiota; CT1, Canditoa 1; CT3, Candiota 3; QUT, Quitéria; GS.1, Ganigobis 1; ZWFUN.1, Zwartbas 1; ZWFUN.2, Zwartbas 2; OG-09, Owl Gorge-09; Prince A. Fm, Prince Albert Formation. Source: stratigraphic framework modified after Griffis *et al.* (2019*a*, 2021).

Paraná Basin confirms an African ice source (Griffis *et al.* 2019*b*; Fedorchuk *et al.* 2021). The anatomy of the deglaciation successions across the Paraná Basin generally involves the juxtaposition of 'deeper water' facies directly on top of the subglacial surfaces and includes finely laminated rhythmites, organic-rich mudstones as well as glacially influenced mass transport deposits (Figs 2 & 3c; Valdez Buso *et al.* 2019; Fedorchuk *et al.* 2019*b*). Generally, one to two deglaciation successions are found in the southern Paraná Basin in Brazil and Uruguay, whereas at least three and as many as five are found along the SE margin of the Paraná Basin (Vesely *et al.* 2015; Mottin *et al.* 2018; Assine *et al.* 2018; Fallgatter and Paim 2019; Fedorchuk *et al.* 2019*b*). The latest glaciogenic deposits, referred to as the Rio Do Sul or Taciba formations, are capped by fluvial sandstones and coals of the lower part of the Rio Bonito Formation (Guatá Group), which often host volcanic ash layers containing zircons that are used to refine interbasinal correlations and calibrate the glaciogenic record (Figs 2 & 3g; Holz *et al.* 2010; Cagliari *et al.* 2016; Griffis *et al.* 2018). The Rio Bonito Formation of the Guatá Group is characterized by a highly dynamic base-level record, which has been correlated to the waxing and waning of higher-latitude glaciation (Griffis *et al.* 2019*a*). The lower part of the Rio Bonito Formation is characterized by fluvial sandstone, estuarine and coal facies, which sit directly on deep-water marine deposits, or are incised into local basement (Holz *et al.* 2010). The Itararé Group–Rio Bonito Formation contact is recognized as a regional sequence boundary that can be traced across the Paraná Basin and that formed as a result of a forced regression (Holz *et al.* 2008; Griffis *et al.* 2019*a*).

The lower part of the Rio Bonito Formation, which directly overlies the glaciogenic facies of the Itararé Group across the Paraná Basin, is rich in volcanic ash deposits. Five of the ash deposits have been dated using high-resolution U–Pb zircon CA-TIMS methods and provide age constraints for the demise of glaciation across this region (Griffis *et al.* 2018; Fig. 2). Three of the U–Pb zircon CA-TIMS ages are from tonsteins (HNC, CT1 and CT3), which are hosted within the coal deposits surrounding the

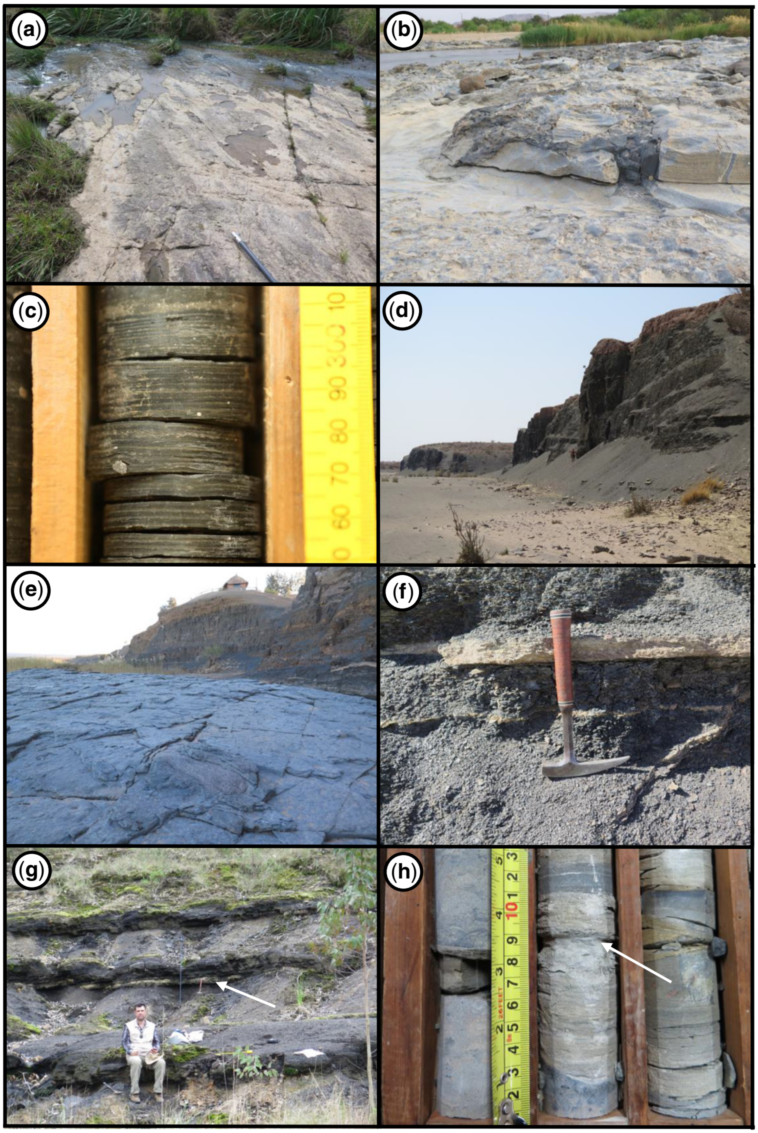

Fig. 3. Photographs of glaciogenic features, black shales and volcanic ash from the uppermost Carboniferous and lower Permian described in this study. (**a**) Striated surface, Cachoeira do Sul, Rio Grande do Sul State, Brazil; 30 cm staff for scale. (**b**) Irregular subglacial Dwyka Group contact with basement along the orange river in the Karasburg sub-basin, outside the town of Noordoewer, Namibia. Rand coin for scale. (**c**) Rhythmites of the Rio do Sul Formation with outsized clasts in the Anitápolis core, Santa Catarina State, Brazil. (**d**) Outcrop of Ganigobis Shale Member; person for scale. (**e**) Glacial diamictite contact with black shales near Zwartbas. Note large, outsized clast in foreground. (**f**) Volcanic ash (GS.1) within the Ganigobis Shale Member. (**g**) Tonstein located in the Candiota coal units outside of Hulha Negra Candiota. Hammer notes stratigraphic horizon of HNC1. (**h**) Volcaniclastic unit (ANT1) within the lower part of the Rio Bonito Formation in the Anitápolis core.

village of Candiota in Rio Grande do Sul State. One age comes from an isolated outcrop (QUT), which is in central Rio Grande do Sul, 150 km NE of Candiota (Figs 2 & 3g). The U–Pb ages from the lower part of the Rio Bonito Formation range from 298.23 ± 0.31 Ma to $296.97 + 0.45/-0.72$ Ma (Griffis *et al.* 2018). An additional U–Pb zircon age of $297.4 + 1.13/-1.19$ Ma was reported from an ash (ANT1) sampled in fluvial deltaic facies located 60 m above the Guatá–Itararé Group contact in the lower part of the Rio Bonito Formation from the Anitápolis core in Santa Catarina State (Figs 2 & 3h; Griffis *et al.* 2019*a*). Importantly, the Anitápolis core contains the same stratigraphy and is located within the vicinity of the palaeovalley successions described by Fallgatter and Paim (2019), confirming a Carboniferous age for the glacial facies in this region (Griffis *et al.* 2018, 2019*a*, 2021).

Kalahari Basin

The Kalahari Basin covers an area greater than 2.5 × 10^6 km^2, extending across Namibia and Botswana as well as parts of Zimbabwe, Zambia, South Africa and Angola (Fig. 1; Visser 1983, 1997; Catuneanu *et al.* 2005). Glaciogenic deposits in southern Africa are constrained to the Dwyka Group (Fig. 2), which occurs in outcrop along the margins of the Kalahari Basin and is found in cores across much of this region (Frakes and Crowell 1970; Visser 1983; Cairncross 2001; Linol *et al.* 2016; Dietrich and Hofmann 2019). The Dwyka Group attains a maximum thickness of 800 m in the Karoo Basin of South Africa, where the group is defined, and reaches a maximum thickness of *c.* 200 m in outcrop across southern Namibia (Fig. 2; Visser 1997; Stollhofen *et al.* 2008). The Dwyka Group records a highly dynamic glaciogenic record, which is divided into four ice advance–retreat cycles, referred to as deglaciation sequences (DS), which are defined in South Africa by a lower subglacial or ice proximal unit that is overlain by deeper water ice-distal or ice-free deposits (Visser 1997; Isbell *et al.* 2008). Marine mudstones of the Ecca Group directly overlie the Dwyka Group deposits and mark the demise of ice in this region (Visser 1997). Deglaciation sequences have been correlated across southern Africa, through high-resolution U–Pb zircon CA-TIMS analysis, challenging some of the previous correlations, as the Kalahari Basin was ice free 12 myr prior to the Karoo Basin (Griffis *et al.* 2021). Here we briefly review some of the subglacial and the immediate postglacial record in the Kalahari Basin as well as the current temporal constraints on the deposits.

Namibia hosts one of the highest fidelity records of the late Paleozoic glaciation, preserving ancient fjord networks, a complex basal unconformity that extends for hundreds of kilometres in outcrop and large linear erosional features including drumlins, which attest to the subglacial history of this region (Figs 2 & 3b; Martin 1981; Andrews *et al.* 2019; Dietrich and Hofmann 2019; Le Heron *et al.* 2021). During the acme of the LPIA a large, at least 1.7 km thick, ice sheet covered northern Namibia (Dietrich *et al.* 2021). Deeply incised palaeovalleys, up to 1 km in depth and 5 km in width, can be traced for tens to hundreds of kilometres and are interpreted to have been carved by an ice sheet that propagated across northern Namibia and into the Paraná Basin (Fallgatter and Paim 2019; Rosa *et al.* 2019; Dietrich *et al.* 2021). Polished and striated surfaces as well as diamictite are found above and outside the valley walls indicating that these regions were overtopped by ice during the acme of the glaciation (Martin 1981; Dietrich *et al.* 2021). Additional scoured and striated surfaces are preserved along the floor and walls of the valleys, with multiple stepped levels of marginal moraine interpreted as recording ice advance–retreat cycles (Dietrich *et al.* 2021). Ultimately, these valleys were filled with marine rocks, and given the scale and well-preserved nature of the deposits are regarded as one of the world's best-preserved examples of a pre-Cenozoic fjord network (Dietrich *et al.* 2021; Le Heron *et al.* 2022). In southern Namibia, equally impressive outcrops within the Aranos and Karasburg sub-basins of the greater Kalahari record a complex system of fluvial incision, subglacial erosion and ice proximal deposits, which unconformably overlie Precambrian–Cambrian basement attesting to the growth and progradation of ice across this region (Stollhofen *et al.* 2008; Le Heron *et al.* 2021). Boulder beds, striated and polished surfaces and subglacial shearing of unconsolidated sediments are documented across these regions and confirm subglacial and proglacial conditions (Figs 2 & 3b, e; Visser 1983; Le Heron *et al.* 2021). The subglacial deposits across southern Namibia are overlain by a distinct 20–50 m thick black shale facies, referred to as the Ganigobis Shale Member (Aranos sub-basin) or Zwartbas shale (Karasburg sub-basin), which represent a major marine transgression, which formed as a result of abrupt ice loss during DSII (Figs 2 & 3d; Werner 2006; Stollhofen *et al.* 2008). These black shales mark the demise of subglacial evidence across this region of Gondwana (Visser 1997; Griffis *et al.* 2021). In addition, the Ganigobis Shale Member incorporates columnar limestone deposits, which are interpreted to have formed around methane seeps (Birgel *et al.* 2008; Himmler *et al.* 2008). At least one glaciogenic horizon occurs above the Ganigobis Shale Member and the correlative shales near Zwartbas (Fig. 2). The final demise of ice in Namibia is associated with the deposition of mudstones from the Ecca Group, which overlies the uppermost glaciogenic rocks.

The Ganigobis Shale Member and the black shales near Zwartbas directly overlie the subglacial facies of the lower part of the Dwyka Group in Namibia and contain volcanic ash layers, which have been dated radioisotopically and provide age control for the disappearance of grounded ice in this region (Werner 2006; Stollhofen *et al.* 2008). High-resolution U–Pb CA-TIMS analyses from three volcanic ash units indicate that the deposition of the black shales was synchronous and constrained to the latest Carboniferous. Two volcanic ashes sampled 5 and 7 m above the subglacial facies of the lower part of the Dwyka Group in the shales near Zwartbas within the Karasburg sub-basin yield ages between 300.45 ± 0.37 and 299.41 ± 0.24 Ma, respectively (Fig. 2). In the Aranos sub-basin, a similar age of 299.31 ± 0.35 Ma was reported from an ash unit sampled in the Ganigobis Shale Member, 5 m above the contact with the underlying glaciogenic facies (Figs 2 & 3f). The reported late Carboniferous ages for the black shales indicate an abrupt latest Carboniferous warming responsible for the demise of subglacial ice in this region. Glacially influenced deposits occur above these shales, in the upper part of the Dwyka Group, including debris flow diamict and dropstones, though no subglacial evidence is found in this region. The final demise of ice in Namibia is constrained by an ash bed (OG-09) dated at 295.84 ± 0.47 Ma, 7 m above the Dwyka Group–Prince Albert Formation contact, in the lower part of the Ecca Group of the Karasburg basin (Fig. 2; Griffis *et al.* 2021).

The upper Paleozoic sedimentary record of the Paraná and Kalahari basins records the transition from subglacial reservoirs to ice-free conditions across SW Gondwana by the latest Carboniferous. During peak glaciation in the Carboniferous, glaciers occupied the mid- to high-latitude continental and upland regions with evidence for dynamic wet-based glaciers occurring along basin margins or near subglacial ice streams (Visser 1983; Fedorchuk *et al.* 2019*b*; Rosa *et al.* 2019; Le Heron *et al.* 2022). Glaciers carved valleys in the upland regions, and ice sheets emanated across southern Africa and into South America (Isbell *et al.* 2012; Assine *et al.* 2018; Fallgatter and Paim 2019; Rosa *et al.* 2019; Fedorchuk *et al.* 2021; Dietrich *et al.* 2021; Le Heron *et al.* 2022). Detrital zircon geochronology from glaciogenic deposits confirms these findings, with zircons with African provenance recovered from Paraná Basin glaciogenic deposits (Griffis *et al.* 2019*b*, 2021; Fedorchuk *et al.* 2021). The latest Carboniferous was associated with an abrupt change in the style and distribution of Gondwanan glaciers, where once-subglacial basins transitioned to 'ice-distal' or non-glacial marine conditions in the Kalahari and Paraná regions. In the Paraná Basin, the Rio Do Sul and Taciba formations contain the last glacially influenced deposits in the region and are temporally correlative with the Ganigobis Shale Member of Namibia (Fig. 2). The demise of glaciers within these basins is coincident with a near doubling of pCO_2, from mid Carboniferous lows to the late Carboniferous, where values are two times present atmospheric level, though forcing mechanisms related to the abrupt release of pCO_2 are unresolved (Richey *et al.* 2020; Montañez 2022).

Abrupt late Carboniferous warming

On the $>10^6$-year timescales, icehouse climate systems are largely driven by changes in the sinks and sources of greenhouse gases. Sinks include silicate weathering in the tropics, deliverability of alkalinity to ocean basins and the burial of organic matter and are counter-balanced by the release of greenhouse gases though processes such as volcanism (McKenzie *et al.* 2016; Nelsen *et al.* 2016; MacDonald *et al.* 2019). The late Carboniferous and early Permian is characterized by a highly variable pCO_2 record, with a late Carboniferous peak (*c.* 304 Ma; 600 ppmv) followed by a nadir in the earliest Permian (*c.* 298 Ma; 200 ppmv; Richey *et al.* 2020). The latest Carboniferous warming is coincident with ocean anoxia and the demise of Gondwanan glaciers, whereas the nadir in the earliest Permian is associated with the return of glaciogenic conditions in regions surrounding the Kalahari and Karoo basins, and lowstand sedimentation in the Paraná Basin (Griffis *et al.* 2019*a*; Chen *et al.* 2022). Punctuated warming events in the late Carboniferous overprint the longer-term trend of decreasing pCO_2 through the early Permian indicating a likely short-lived, high-volume release of greenhouse gas that overprints the longer-term ($>10^6$-year) sink, the latter of which is attributed to weathering (Richey *et al.* 2020).

Drivers for the abrupt demise of the Gondwanan ice are unresolved in the latest Carboniferous. Degassing as a result volcanism is postulated as a main driver for late Paleozoic deglaciation (McKenzie *et al.* 2016; Yang *et al.* 2020), whereas other studies invoke volcanism as the main driver of glaciation, caused by negative radiative forcing associated with the release of aerosol particles into the stratosphere and an increased ocean biological pump driven by the fertilization of ocean basins (Soreghan *et al.* 2019). Constraints on the age and tempo of the proposed drivers are limited to the $>10^6$-year timescale, an order of magnitude less precise then the pCO_2 and ice records from this time period, making it difficult to resolve processes responsible for the demise of glaciation and which ultimately highlights the need for additional geochronological constraints on glaciogenic deposits and volcanic sources. Lastly, we discuss other possible greenhouse gas sources, such as methane seeps, which may have contributed to the amplification of late Paleozoic deglaciations (Himmler *et al.* 2008; Haig *et al.* 2022).

The synchronous demise of glaciers in the latest Carboniferous at *c.* 300 Ma in the Kalahari and Paraná basins requires a high-volume, short-duration release of greenhouse gases. The Skagerrak Centred Large Igneous Province has been proposed as a possible driver (Griffis 2018; Yang *et al.* 2020), though current temporal constraints on the Skagerrak

Centred Large Igneous Province are coarse, precluding our ability to directly correlate these events. As an example, a current pooled age of 297 ± 4 Ma (weighted mean; Torsvik *et al.* 2008) for all volcanic intrusions and eruptions of the Skagerrak Centred Large Igneous Province indicate anywhere between a latest Carboniferous through early Permian record for emplacement. Importantly, a 300–299 Ma age for the top of DSII is congruent with the eruption, as is the return of ice at 298 Ma and DSIII (296 Ma), and therefore deciphering whether the Skagerrak Centred Large Igneous Province was an actual driver of deglaciation, or possibly the glaciation, is unattainable given that the temporal constraints and quoted uncertainties permit either interpretation.

A volcanic driver of glaciation has also been proposed for the late Paleozoic based on inconsistencies between the pCO_2 and the ice record, where an earliest Permian peak in glaciogenic deposits is coincident with a peak in global volcanic activity (Soreghan *et al.* 2019). In this scenario, volcanic aerosols are released into the stratosphere resulting in negative radiative forcing, which was further amplified by fertilizing ocean basins with reactive iron, resulting in an increased biological pump and carbon sequestration. This hypothesis requires an unprecedented scale and tempo of volcanism given the short residence time of aerosol particles in the stratosphere (cf. Lee and Dee 2019). Foundational to the volcanic driver hypothesis is a disconnect between pCO_2 and the ice record, though recent studies have confirmed this connection, where periods of elevated pCO_2 in the latest Carboniferous are contemporaneous with widespread ice loss (Griffis *et al.* 2019*a*, 2021; Richey *et al.* 2020). The volcanic driver hypothesis also assumes an early Permian apex (298–295 Ma) for the late Paleozoic glaciation, which was established based on the global frequency of glacial diamictites across the LPIA (cf. Soreghan *et al.* 2019). The frequency of diamictites as a proxy for a glacial maximum is limited by the poor temporal constraints on the glaciogenic deposits and the nature, preservation and representation of the diamict, i.e. ice contact, ice-distal deposits or non-glacial origin (Fedorchuk *et al.* 2019*a*; Dietrich and Hofmann 2019). The presence of diamictite deposits within a basin does not require glaciogenic conditions. In fact, detailed field and sedimentological evidence has shown in many instances that these deposits may have a non-glacial origin or represent mass transport and/or slope failure deposits associated with ice collapse (Dietrich and Hofmann 2019; Fedorchuk *et al.* 2019*b*; Rosa *et al.* 2019). Furthermore, glaciogenic deposits during the late Paleozoic are likely biased towards the demise of the ice record, a result in changes in accommodation space and the nature of glacial processes, and therefore the maximum occurrence of diamictites does not correlate with peak ice (González-Bonorino and Eyles 1995). The presented histories of the Paraná and Kalahari basins indicate that all subglacial evidence in these basins is constrained to the Carboniferous, not early Permian, and given the size and latitudinal extents, argues against an early Permian apex for late Paleozoic ice.

In the Kalahari Basin, the widespread occurrence of columnar limestones beds, which formed through microbial activity around hydrocarbon seeps, are associated with the immediate postglacial deposits of the Ganigobis Shale Member (Birgel *et al.* 2008; Himmler *et al.* 2008). Similar columnar limestone facies formed around hydrocarbon seeps in black shales in western Australia, directly above glaciogenic deposits in the lower Permian (Sakmarian) Holmwood Shale (Haig *et al.* 2022). In these basins, the limestone columns formed in response to the anaerobic oxidation of methane, evidenced by $\delta^{13}C$ values as depleted as −51‰ (Birgel *et al.* 2008). Importantly, these deposits are also documented in the Cretaceous of the Canadian Arctic, where they are attributed as a driver between cold to warm climate conditions in the latest Albian (Williscroft *et al.* 2017). Whereas the spatial distribution of methane seeps is not resolved in the late Paleozoic, the immediate occurrence with deglacial black shales merits further investigation, especially given the outsized influence of methane as a greenhouse gas, which is 25 times more potent than CO_2 (Yvon-Durocher *et al.* 2014).

The Carboniferous apex

Detailed field studies of glaciogenic reservoirs coupled with recently published high-resolution U–Pb zircon CA-TIMS geochronological constraints from across the Paraná and Kalahari basins indicate subglacial evidence in these two massive intracratonic basins, which span between 45° and 65° S latitude, is restricted to the Carboniferous (Vesely *et al.* 2018; Fallgatter and Paim 2019; Fedorchuk *et al.* 2019*b*; Griffis *et al.* 2019*a*, 2021; Rosa *et al.* 2019; Le Heron *et al.* 2022). A Carboniferous apex for the late Paleozoic glaciation in southern Gondwana is incongruent with the accepted early Permian peak. The early Permian apex was established based on the secondary ion mass spectrometry (SIMS) U–Pb zircon calibrated eastern Australian ice record, which indicates maximum ice extent in the early Permian, referred to as (P-1), and stable isotope records from across the low latitudes, which show an enrichment in $\delta^{18}O$ at this time (Fielding *et al.* 2008; Koch and Frank 2011). Additional evidence for an early Permian apex of LPIA glaciation includes the abrupt juxtaposition of terrestrial successions on marine platforms in the Pangaean tropics and the occurrence of widespread silt deposition, which is attributed to upland glaciers (Koch and Frank 2011; Soreghan *et al.* 2014, 2019; Pfeifer *et al.* 2021). In contrast, evidence for a Carboniferous peak is based on the zircon U–Pb CA-TIMS calibrated record from southern Gondwanan glaciogenic deposits, the cyclothem records from the mid-continent of the United States and Europe, which are widespread in the Carboniferous and diminish by the early Permian, as well as conodont apatite $\delta^{18}O$ oxygen isotope enrichment in the Bashkirian from the Nanjing section of China, interpreted as the late Paleozoic glacial maximum (Heckel 1977, 2008; Gulbranson *et al.* 2010; Buggisch *et al.* 2011; Eros *et al.* 2012; Chen *et al.* 2016; Griffis *et al.* 2018, 2019*a*, 2021).

Reconciling these records and their interpretations is required to gain a better understanding as to the timing and forcing mechanisms responsible for the demise of the LPIA. The Australian glaciogenic record is regarded as one of the best-preserved upper Paleozoic deposits and is often used to define the Paleozoic glaciogenic periods (Fielding *et al.* 2008). The age control used to build this framework is largely based on *in situ* analytical techniques on zircons that were not treated for Pb loss and in part compromised by the use of calibration standards that are now known to be heterogeneous (Black *et al.* 2003). Therefore, new high-precision U–Pb zircon age constraints from Australia are needed to test current stratigraphic assignments. To that extent the U–Pb CA-TIMS calibrated record of the LPIA for southern and western Gondwana is the most precise and accurate temporal framework of late Paleozoic glaciation and is congruent with a Carboniferous peak (Gulbranson *et al.* 2010; Griffis *et al.* 2019*a*, 2021). In addition, the low-latitude evidence for glaciation may have more parsimonious non-glacial interpretations. The Unaweep canyon in western Colorado, previously interpreted as an exhumed glacial valley (Soreghan *et al.* 2008, 2014), has been reinterpreted as an exhumed fluvial valley formed through the uplift of the Uncompahgre Plateau in the Cenozoic (Hood *et al.* 2009; Rønnevik *et al.* 2017). Widespread silt deposition across the Pangaean tropics in the early Permian has also been argued as evidence for upland glaciation in the Central Pangaea Mountains (Soreghan *et al.* 2014; Pfeifer *et al.* 2021). Radioisotopic age constraints for the silt deposits are lacking in North America, though in the Lodève Basin of France are well constrained to the Sakmarian–Artinskian based on U–Pb zircon maximum depositional ages from zircon recovered in the silts and high-precision U–Pb CA-TIMS from volcaniclastic units (Michel *et al.* 2015; Pfeifer *et al.* 2021). Importantly, the early Permian was a period of widespread ice loss in polar Gondwana, which was accompanied by the onset of aridification in the tropics as evidenced by the diversification of drought tolerant plants, palaeosols enriched in carbonate and smectite clays, and a rise in pCO_2 (Tabor *et al.* 2013; Griffis *et al.* 2019*a*, 2023; Richey *et al.* 2020; Marchetti *et al.* 2022). The lack of any definitive ice contact deposits in the Pangaean tropics, coupled with high-latitude ice loss in the early Permian and aridification across this region suggests a likely non-glacial origin for the silt.

Conclusions

The Paraná and Kalahari basins of southern Gondwana preserve one of the most extensive and best-calibrated records of the late Paleozoic glaciation. Subglacial landforms, which include fjord networks, striated pavements and roche moutonnée, as well as subglacial or ice contact deposits such as boulder beds and push moraine complexes, formed through erosional possesses associated with the expansion of ice sheets and upland glaciers across these regions in the Carboniferous. An acute climatic amelioration occurred in the latest Carboniferous, which is evidenced by the abrupt loss of glaciogenic rocks and the onset of marine conditions in these basins. High-precision U–Pb zircon CA-TIMS geochronological constraints from volcaniclastic units hosted within the marine shales of Namibia and in fluvial and coal deposits, which overlie the glaciogenic rocks in the Paraná Basin, indicate that these basins were ice free in the latest Carboniferous (*c.* 300 Ma). Importantly, no subglacial evidence is documented in the basins following the late Carboniferous warming, though glaciogenic rocks persist in Namibia through the early Permian (296 Ma). The abrupt and synchronous loss of glaciogenic rocks in southern Gondwana occurred in tandem with a short-lived rise in pCO_2. The unrecoverable loss of subglacial ice in the late Carboniferous, despite a return to low pCO_2 in the earliest Permian, suggests an ice threshold had been crossed in the late Carboniferous and requires a short-term driver of greenhouse gases, such as volcanism. The loss of grounded ice in these basins by the late Carboniferous suggests the apex of the late Paleozoic icehouse is in the Carboniferous.

Acknowledgements I would like to thank Spencer Lucas, Bill DiMichele, Cortland Eble and Stanislav Opluštil for constructive feedback on this manuscript. Any use of trade, firm or product names is for descriptive purposes only and does not imply endorsement by the US Government.

Competing interests The authors declare that they have no known competing financial interests or personal relationships that could have appeared to influence the work reported in this paper.

Author contributions **NG**: conceptualization (lead), writing – original draft (lead); **RM**: conceptualization (supporting), writing – review & editing (supporting); **IM**: conceptualization (supporting), writing – review & editing (supporting); **DLH**: conceptualization (supporting); **PD**: conceptualization (supporting); **RI**: conceptualization (supporting).

Funding This research received no specific grant from any funding agency in the public, commercial or not-for-profit sectors.

Data availability Data sharing is not applicable to this article as no datasets were generated or analysed during the current study.

References

Andrews, G.D., McGrady, A.T., Brown, S.R. and Maynard, S.M. 2019. First description of subglacial megalineations from the late Paleozoic ice age in Southern Africa. *PLoS ONE*, **14**, e0210673, https://doi.org/10.1371/journal.pone.0210673

Assine, M.L., de Santa Ana, H., Veroslavsky, G. and Vesely, F.F. 2018. Exhumed subglacial landscape in Uruguay: erosional landforms, depositional environments, and paleo-ice flow in the context of the late Paleozoic Gondwanan glaciation. *Sedimentary Geology*, **369**, 1–12, https://doi.org/10.1016/j.sedgeo.2018.03.011

Bangert, B., Stollhofen, H., Lorenz, V. and Armstrong, R.L. 1999. The geochronology and significance of ash-fall tuffs in the glaciogenic Carboniferous-Permian Dwyka Group of Namibia and South Africa. *Journal of African Earth Sciences*, **29**, 33–49, https://doi.org/10.1016/S0899-5362(99)00078-0

Birgel, D., Himmler, T., Freiwald, A. and Peckmann, J. 2008. A new constraint on the antiquity of anaerobic oxidation of methane: Late Pennsylvanian seep limestones from southern Namibia. *Geology*, **36**, 543–546, https://doi.org/10.1130/g24690a.1

Black, L.P., Kamo, S.L., Williams, I.S., Mundil, R., Davis, D.W., Korsch, R.J. and Foudoulis, C. 2003. The application of SHRIMP to Phanerozoic geochronology; a critical appraisal of four zircon standards. *Chemical Geology*, **200**, 171–188, https://doi.org/10.1016/s0009-2541(03)00166-9

Buggisch, W., Wang, X., Alekseev, A.S. and Joachimski, M.M. 2011. Carboniferous–Permian carbon isotope stratigraphy of successions from China (Yangtze platform), USA (Kansas) and Russia (Moscow basin and Urals). *Palaeogeography, Palaeoclimatology, Palaeoecology*, **301**, 18–38, https://doi.org/10.1016/j.palaeo.2010.12.015

Cagliari, J., Philipp, R.P. *et al*. 2016. Age constraints of the glaciation in the Paraná Basin: evidence from new U–Pb dates. *Journal of the Geological Society, London*, **173**, 871–874, https://doi.org/10.1144/jgs2015-161

Cairncross, B. 2001. An overview of the Permian (Karoo) coal deposits of Southern Africa. *Journal of African Earth Sciences*, **33**, 529–562, https://doi.org/10.1016/s0899-5362(01)00088-4

Catuneanu, O., Wopfner, H., Eriksson, P.G., Cairncross, B., Rubidge, B.S., Smith, R.M.H. and Hancox, P.J. 2005. The Karoo basins of south-Central Africa. *Journal of African Earth Sciences*, **43**, 211–253, https://doi.org/10.1016/j.jafrearsci.2005.07.007

Chen, B., Joachimski, M.M., Wang, X.-D., Shen, S.-Z., Qi, Y.-P. and Qie, W.-K. 2016. Ice volume and paleoclimate history of the late Paleozoic ice age from conodont apatite oxygen isotopes from Naqing (Guizhou, China). *Palaeogeography, Palaeoclimatology, Palaeoecology*, **448**, 151–161, https://doi.org/10.1016/j.palaeo.2016.01.002

Chen, J., Montañez, I.P. *et al*. 2022. Marine anoxia linked to abrupt global warming during Earth's penultimate Icehouse. *Proceedings of the National Academy of Sciences*, **119**, e2115231119, https://doi.org/10.1073/pnas.2115231119

Cleal, C.J. and Thomas, B.A. 2005. Palaeozoic tropical rainforests and their effect on global climates: is the past the key to the present? *Geobiology*, **3**, 13–31, https://doi.org/10.1111/j.1472-4669.2005.00043.x

Dietrich, P. and Hofmann, A. 2019. Ice-margin fluctuation sequences and grounding zone wedges: the record of the Late Paleozoic Ice Age in the eastern Karoo Basin (Dwyka Group, South Africa). *The Depositional Record*, **5**, 247–271, https://doi.org/10.1002/dep2.74

Dietrich, P., Griffis, N.P., Le Heron, D.P., Montañez, I.P., Kettler, C., Robin, C. and Guillocheau, F. 2021. Fjord network in Namibia: a snapshot into the dynamics of the late Paleozoic glaciation. *Geology*, **49**, 1521–1526, https://doi.org/10.1130/g49067.1

Eros, J.M., Montañez, I.P., Osleger, D.A., Davydov, V.I., Nemyrovska, T.I., Poletaev, V.I. and Zhykalyak, M.V. 2012. Sequence stratigraphy and onlap history of the Donets Basin, Ukraine: insight into Carboniferous icehouse dynamics. *Palaeogeography, Palaeoclimatology, Palaeoecology*, **313–314**, 1–25, https://doi.org/10.1016/j.palaeo.2011.08.019

Eyles, C.H., Eyles, N. and Franca, A.B. 1993. Glaciation and tectonics in an active intracratonic basin: the late Palaeozoic Itararé group, Paraná Basin, Brazil. *Sedimentology*, **40**, 1–25, https://doi.org/10.1111/j.1365-3091.1993.tb01087

Fallgatter, C. and Paim, P.S.G. 2019. On the origin of the Itararé Group basal nonconformity and its implications for the late Paleozoic glaciation in the Paraná Basin, Brazil. *Palaeogeography, Palaeoclimatology, Palaeoecology*, **531**, 108225, https://doi.org/10.1016/j.palaeo.2017.02.039

Fedorchuk, N.D., Isbell, J.L. *et al*. 2019*a*. Origin of paleovalleys on the Rio Grande do Sul Shield (Brazil): implications for the extent of late Paleozoic glaciation in west-central Gondwana. *Palaeogeography, Palaeoclimatology, Palaeoecology*, **531**, 108738, https://doi.org/10.1016/j.palaeo.2018.04.013

Fedorchuk, N.D., Isbell, J.L. *et al*. 2019*b*. Carboniferous glaciotectonized sediments in the southernmost Paraná Basin, Brazil: ice marginal dynamics and paleoclimate indicators. *Sedimentary Geology*, **389**, 54–72, https://doi.org/10.1016/j.sedgeo.2019.05.006

Fedorchuk, N.D., Griffis, N.P. *et al*. 2021. Provenance of late Paleozoic glacial/post-glacial deposits in the eastern Chaco-Paraná Basin, Uruguay and southernmost Paraná Basin, Brazil. *Journal of South American Earth Sciences*, **106**, 102989, https://doi.org/10.1016/j.jsames.2020.102989

Fielding, C.R., Frank, T.D. and Isbell, J.L. 2008. The late Paleozoic ice age – a review of current understanding and synthesis of global climate patterns. *Geological Society of America Special Papers*, **441**, 343–354, https://doi.org/10.1130/2008.2441(24)

Frakes, L.A. and Crowell, J.C. 1970. Late Paleozoic glaciation: II. Africa, exclusive of the Karoo Basin. *Geological Society of America Bulletin*, **81**, 2261–2286, https://doi.org/10.1130/0016-7606(1970)81[2261:LPGIAE]2.0.CO;2

Gastaldo, R.A., DiMichele, W.A. and Pfefferkorn, H.W. 1996. Out of the icehouse into the greenhouse; a late Paleozoic analog for modern global vegetational change. *GSA Today*, **6**, 1–7.

Gesicki, A.L.D., Riccomini, C. and Boggiani, P.C. 2002. Ice flow direction during late Paleozoic glaciation in western Paraná Basin, Brazil. *Journal of South American Earth Sciences*, **14**, 933–939, https://doi.org/10.1016/S0895-9811(01)00076-1

González-Bonorino, G. and Eyles, N. 1995. Inverse relation between ice extent and the late Paleozoic glacial record of Gondwana. *Geology*, **23**, 1015–1018, https://doi.org/10.1130/0091-7613(1995)023<1015:irbiea>2.3.co;2

Griffis, N. 2018. *From Isotopes to Ice: Refining the late Paleozoic Glaciation in Time and Space*. PhD thesis, University of California, Davis, 114.

Griffis, N.P., Mundil, R. *et al*. 2018. A new stratigraphic framework built on U–Pb single-zircon TIMS ages and implications for the timing of the penultimate icehouse (Paraná Basin, Brazil). *Geological Society of America Bulletin*, **130**, 848–858, https://doi.org/10.1130/B31775.1

Griffis, N.P., Montañez, I.P. *et al*. 2019*a*. Coupled stratigraphic and U–Pb zircon age constraints on the late Paleozoic icehouse-to-greenhouse turnover in south-central Gondwana. *Geology*, **47**, 1146–1150, https://doi.org/10.1130/g46740.1

Griffis, N.P., Montañez, I.P. *et al*. 2019*b*. Isotopes to ice: constraining provenance of glacial deposits and ice centers in west-central Gondwana. *Palaeogeography, Palaeoclimatology, Palaeoecology*, **531**, 108745, https://doi.org/10.1016/j.palaeo.2018.04.020

Griffis, N., Montañez, I. *et al*. 2021. High-latitude ice and climate control on sediment supply across SW Gondwana during the late Carboniferous and early Permian. *Geological Society of America Bulletin*, **133**, 2113–2124, https://doi.org/10.1130/b35852.1

Griffis, N., Tabor, N., Stockli, D. and Stockli, L. 2023. The Far-Field imprint of the late Paleozoic Ice Age, its demise, and the onset of a dust-house climate across the Eastern Shelf of the Midland Basin, Texas. *Gondwana Research*, **115**, 17–36, https://doi.org/10.1016/j.gr.2022.11.004

Gulbranson, E.L., Montanez, I.P., Schmitz, M.D., Limarino, C.O., Isbell, J.L., Marenssi, S.A. and Crowley, J.L. 2010. High-precision U–Pb calibration of Carboniferous glaciation and climate history, Paganzo Group, NW Argentina. *Geological Society of America Bulletin*, **122**, 1480–1498, https://doi.org/10.1130/B30025.1

Haig, D.W., Dillinger, A. *et al*. 2022. Methane seeps following early Permian (Sakmarian) deglaciation, Interior East Gondwana, Western Australia: multiphase carbonate cements, distinct carbon-isotope signatures, extraordinary biota. *Palaeogeography, Palaeoclimatology, Palaeoecology*, **591**, 110862, https://doi.org/10.1016/j.palaeo.2022.110862

Heckel, P.H. 1977. Origin of phosphatic black shale facies in Pennsylvanian cyclothems of Mid-Continent North America. *AAPG Bulletin*, **61**, 1045–1068, https://doi.org/10.1306/c1ea43c4-16c9-11d7-8645000102c1865d

Heckel, P.H. 2008. Pennsylvanian cyclothems in Midcontinent North America as far-field effects of waxing and waning of Gondwana Ice Sheets. *Geological Society of America Special Papers*, **441**, 275–289, https://doi.org/10.1130/2008.2441(19)

Himmler, T., Freiwald, A., Stollhofen, H. and Peckmann, J. 2008. Late Carboniferous hydrocarbon-seep carbonates from the glaciomarine Dwyka Group, southern Namibia. *Palaeogeography, Palaeoclimatology, Palaeoecology*, **257**, 185–197, https://doi.org/10.1016/j.palaeo.2007.09.018

Holz, M., Souza, P.A. and Iannuzzi, R. 2008. Sequence stratigraphy and biostratigraphy of the Late Carboniferous to Early Permian glacial succession (Itararé Subgroup) at the eastern southeastern margin of the Paraná Basin, Brazil. *Geological Society of America Special Papers*, **441**, 115–129, https://doi.org/10.1130/2008.2441(08)

Holz, M., Franca, A.B., Souza, P.A., Iannuzzi, R. and Rohn, R. 2010. A stratigraphic chart of the Late Carboniferous/Permian succession of the eastern border of the Paraná Basin, Brazil, South America. *Journal of South American Earth Sciences*, **29**, 381–399, https://doi.org/10.1016/j.jsames.2009.04.004

Hood, W., Cole, R. and Aslan, A. 2009. Anomalous cold in the Pangaean tropics: comment. *Geology*, **37**, e192, https://doi.org/10.1130/G30035C.1

Isbell, J.L., Miller, M.F., Wolfe, K.L. and Lenaker, P.A. 2003. Timing of late Paleozoic glaciation in Gondwana: was glaciation responsible for the development of northern hemisphere cyclothems? *Geological Society of America Special Papers*, **370**, 5–24, https://doi.org/10.1130/0-8137-2370-1.5

Isbell, J.L., Cole, D.I. and Catuneanu, O. 2008. Carboniferous-Permian glaciation in the main Karoo Basin, South Africa: stratigraphy, depositional controls, and glacial dynamics. *Geological Society of America Special Papers*, **441**, 71–82, https://doi.org/10.1130/2008.2441(05)

Isbell, J.L., Henry, L.C. *et al*. 2012. Glacial paradoxes during the late Paleozoic ice age: evaluating the equilibrium line altitude as a control on glaciation. *Gondwana Research*, **22**, 1–19, https://doi.org/10.1016/j.gr.2011.11.005

Koch, J.T. and Frank, T.D. 2011. The Pennsylvanian–Permian transition in the low-latitude carbonate record and the onset of major Gondwanan glaciation. *Palaeogeography, Palaeoclimatology, Palaeoecology*, **308**, 362–372, https://doi.org/10.1016/j.palaeo.2011.05.041

Lee, C.-T.A. and Dee, S. 2019. Does volcanism cause warming or cooling? *Geology*, **47**, 687–688, https://doi.org/10.1130/focus072019.1

Le Heron, D.P., Kettler, C. *et al*. 2021. The late Palaeozoic Ice Age unconformity in southern Namibia viewed as a patchwork mosaic. *The Depositional Record*, **8**, 419–435, https://doi.org/10.1002/dep2.163

Le Heron, D.P., Busfield, M.E. *et al*. 2022. New perspectives on glacial geomorphology in Earth's deep time record. *Frontiers in Earth Science*, **10**, https://doi.org/10.3389/feart.2022.870359

Linol, B., de Wit, M.J., Barton, E., de Wit, M.M. and Guillocheau, F. 2016. U–Pb detrital zircon dates and source provenance analysis of Phanerozoic sequences of the Congo Basin, central Gondwana. *Gondwana Research*, **29**, 208–219, https://doi.org/10.1016/j.gr.2014.11.009

López-Gamundí, O., Limarino, C.O., Isbell, J.L., Pauls, K., Césari, S.N. and Alonso-Muruaga, P.J. 2021. The late Paleozoic ice age along the southwestern margin of Gondwana: facies models, age constraints, correlation and sequence stratigraphic framework. *Journal of South American Earth Sciences*, **107**, 103056, https://doi.org/10.1016/j.jsames.2020.103056

Macdonald, F.A., Swanson-Hysell, N.L., Park, Y., Lisiecki, L. and Jagoutz, O. 2019. Arc-continent collisions in the tropics set Earth's climate state. *Science (New York, NY)*, **364**, 181–184, https://doi.org/10.1126/science.aav5300

Marchetti, L., Forte, G. *et al*. 2022. The Artinskian warming event: an Euramerican change in climate and the terrestrial biota during the early Permian. *Earth-Science Reviews*, **226**, 103922, https://doi.org/10.1016/j.earscirev.2022.103922

Martin, H. 1981. The late Palaeozoic Dwyka Group of the South Kalahari Basin in Namibia and Botswana and the subglacial valleys of the Kaokoveld in Namibia. *In*: Hambrey, M.J. and Harland, W.B. (eds) *Earth's Pre-Pleistocene Glacial Record*. Cambridge University Press, Cambridge, UK, 61–66.

McKenzie, N.R., Horton, B.K., Loomis, S.E., Stockli, D.F., Planavsky, N.J. and Lee, C.-T.A. 2016. Continental arc volcanism as the principal driver of icehouse-greenhouse variability. *Science (New York, NY)*, **352**, 444–447, https://doi.org/10.1126/science.aad5787

Michel, L.A., Tabor, N.J., Montañez, I.P., Schmitz, M.D. and Davydov, V.I. 2015. Chronostratigraphy and paleoclimatology of the Lodève Basin, France: evidence for a pan-tropical aridification event across the Carboniferous–Permian boundary. *Palaeogeography, Palaeoclimatology, Palaeoecology*, **430**, 118–131, https://doi.org/10.1016/j.palaeo.2015.03.020

Milani, E.J. and De Wit, M.J. 2008. Correlations between the classic Paraná and Cape–Karoo sequences of South America and Southern Africa and their basin infills flanking the Gondwanides: Du Toit revisited. *Geological Society, London, Special Publications*, **294**, 319–342, https://doi.org/10.1144/sp294.17

Montañez, I.P. 2022. Current synthesis of the penultimate Icehouse and its imprint on the Upper Devonian through Permian stratigraphic record. *Geological Society, London, Special Publications*, **512**, 213–245, https://doi.org/10.1144/sp512-2021-124

Montañez, I.P. and Poulsen, C.J. 2013. The late Paleozoic ice age: an evolving paradigm. *Annual Review of Earth and Planetary Sciences*, **41**, 629–656, https://doi.org/10.1146/annurev.earth.031208.100118

Montañez, I.P., McElwain, J.C. *et al*. 2016. Climate, pCO_2 and terrestrial carbon cycle linkages during late Palaeozoic glacial-interglacial cycles. *Nature Geoscience*, **9**, 824–828, https://doi.org/10.1038/ngeo2822

Mottin, T.E., Vesely, F.F., Rodrigues, M.C.N.L., Kipper, F. and Souza, P.A. 2018. The paths and timing of late Paleozoic ice revisited: new stratigraphic and paleo-ice flow interpretations from a glacial succession in the upper Itararé Group (Paraná Basin, Brazil). *Palaeogeography, Palaeoclimatology, Palaeoecology*, **490**, 488–504, https://doi.org/10.1016/j.palaeo.2017.11.031

Nelsen, M.P., DiMichele, W.A., Peters, S.E. and Boyce, C.K. 2016. Delayed fungal evolution did not cause the Paleozoic peak in coal production. *Proceedings of the National Academy of Sciences*, **113**, 2442–2447, https://doi.org/10.1073/pnas.1517943113

Pfeifer, L.S., Soreghan, G.S., Pochat, S. and Van Den Driessche, J. 2021. Loess in eastern equatorial Pangea archives a dusty atmosphere and possible upland glaciation. *Geological Society of America Bulletin*, **133**, 379–392, https://doi.org/10.1130/b35590.1

Richey, J.D., Montañez, I.P., Godderis, Y., Looy, C.V., Griffis, N.P. and DiMichele, W.A. 2020. Influence of temporally varying weatherability on CO_2–climate coupling and ecosystem change in the late Paleozoic. *Climates of the Past*, **16**, 1759–2020, https://doi.org/10.5194/cp-16-1759-2020

Rocha-Campos, A.C., dos Santos, P.R. and Canuto, J.R. 2008. Late Paleozoic glacial deposits of Brazil: Paraná basin. *Geological Society of America Special Papers*, **441**, 97–114, https://doi.org/10.1130/2008.2441(07)

Rønnevik, C., Ksienzyk, A.K., Fossen, H. and Jacobs, J. 2017. Thermal evolution and exhumation history of the Uncompahgre Plateau (northeastern Colorado Plateau), based on apatite fission track and (U–Th)-He thermochronology and zircon U–Pb dating. *Geosphere*, **13**, 518–537, https://doi.org/10.1130/ges01415.1

Rosa, E.L., Vesely, F.F. and França, A.B. 2016. A review on late Paleozoic ice-related erosional landforms in the Paraná Basin: origin and paleogeographical implications. *Brazilian Journal of Geology*, **46**, 147–166, https://doi.org/10.1590/2317-4889201620160050

Rosa, E.L.M., Vesely, F.F., Isbell, J.I., Kipper, F., Fedorchuk, N.D. and Souza, P.A. 2019. Constraining the timing, kinematics and cyclicity of Mississippian–Early Pennsylvanian glaciations in the Paraná Basin, Brazil. *Sedimentary Geology*, **384**, 29–49, https://doi.org/10.1016/j.sedgeo.2019.03.001

Soreghan, G.S., Soreghan, M.J., Poulsen, C.J., Young, R.A., Eble, C.F., Sweet, D.E. and Davogustto, O.C. 2008. Anomalous cold in the Pangaean tropics. *Geology* , **36**, 659–662, https://doi.org/10.1130/g24822a.1

Soreghan, G.S., Sweet, D.E. and Heavens, N.G. 2014. Upland glaciation in tropical Pangaea: geologic evidence and implications for late Paleozoic climate modeling. *The Journal of Geology*, **122**, 137–163, https://doi.org/10.1086/675255

Soreghan, G.S., Soreghan, M.J. and Heavens, N.G. 2019. Explosive volcanism as a key driver of the late Paleozoic ice age. *Geology*, **47**, 600–604, https://doi.org/10.1130/G46349.1

Stollhofen, H., Werner, M., Stanistreet, I.G. and Armstrong, R.A. 2008. Single-zircon U–Pb dating of

Carboniferous-Permian tuffs, Namibia, and the intercontinental deglaciation cycle framework. *Geological Society of America Special Papers*, **441**, 83–96, https://doi.org/10.1130/2008.2441(06)

Tabor, N.J., DiMichele, W.A., Montañez, I.P. and Chaney, D.S. 2013. Late Paleozoic continental warming of a cold tropical basin and floristic change in Western Pangea. *International Journal of Coal Geology*, **119**, 177–186, https://doi.org/10.1016/j.coal.2013.07.009

Tomazelli, L.J. and Soliani Júnior, E. 1997. Sedimentary facies and depositional environments related to Gondwana glaciation in Batovi and Suspiro regions, Rio Grande do Sul, Brazil. *Journal of South American Earth Sciences*, **10**, 295–303, https://doi.org/10.1016/S0895-9811(97)00019-9

Torsvik, T., Smethurst, M., Burke, K. and Steinberger, B. 2008. Long term stability in deep mantle structure: evidence from the ~300 Ma Skagerrak-Centered Large Igneous Province (the SCLIP). *Earth and Planetary Science Letters*, **267**, 444–452, https://doi.org/10.1016/j.epsl.2007.12.004

Valdez Buso, V., Aquino, C.D. *et al*. 2019. Late Palaeozoic glacial cycles and subcycles in western Gondwana: correlation of surface and subsurface data of the Paraná Basin, Brazil. *Palaeogeography, Palaeoclimatology, Palaeoecology*, **531**, 108435, https://doi.org/10.1016/j.palaeo.2017.09.004

Vesely, F.F., Trzaskos, B., Kipper, F., Assine, M.L. and Souza, P.A. 2015. Sedimentary record of a fluctuating ice margin from the Pennsylvanian of western Gondwana; Paraná Basin, southern Brazil. *Sedimentary Geology*, **326**, 45–63, https://doi.org/10.1016/j.sedgeo.2015.06.012

Vesely, F.F., Rodrigues, M.C.N.L., da Rosa, E.L.M., Amato, J.A., Trzaskos, B., Isbell, J.L. and Fedorchuk, N.D. 2018. Recurrent emplacement of non-glacial diamictite during the Late Paleozoic Ice Age. *Geology* , **46**, 615–618, https://doi.org/10.1130/g45011.1

Visser, J.N.J. 1983. An analysis of the Permo-Carboniferous glaciation in the Marine Kalahari Basin, Southern Africa. *Palaeogeography, Palaeoclimatology, Palaeoecology*, **44**, 295–315, https://doi.org/10.1016/0031-0182(83)90108-6

Visser, J.N.J. 1987. The palaeogeography of part of southwestern Gondwana during the Permo-carboniferous glaciation. *Palaeogeography, Palaeoclimatology, Palaeoecology*, **61**, 205–219, https://doi.org/10.1016/0031-0182(87)90050-2

Visser, J.N.J. 1997. Deglaciation sequences in the Permo-Carboniferous Karoo and Kalahari basins of Southern Africa; a tool in the analysis of cyclic glaciomarine basin fills. *Sedimentology*, **44**, 507–521, https://doi.org/10.1046/j.1365-3091.1997.d01-35.x

Werner, M. 2006. *The Stratigraphy, Sedimentology, and Age of the Late Palaeozoic Mesosaurus Inland Sea, SW Gondwana – New Implications from Studies on Sediments and Altered Pyroclastic Layers of the Dwyka and Ecca Group (Lower Karoo Supergroup) in Southern Namibia*. PhD thesis, University of Würzburg, Würzburg, 425, http://www.opus-bayern.de/uni-wuerzburg/volltexte/2007/2175/

Williscroft, K., Grasby, S.E. *et al*. 2017. Extensive Early Cretaceous (Albian) methane seepage on Ellef Ringnes Island, Canadian High Arctic. *Geological Society of America Bulletin*, **129**, 788–805, https://doi.org/10.1130/b31601.1

Yang, J., Cawood, P.A. *et al*. 2020. Enhanced continental weathering and large igneous province induced climate warming at the Permo-Carboniferous transition. *Earth and Planetary Science Letters*, **534**, 116074, https://doi.org/10.1016/j.epsl.2020.116074

Yvon-Durocher, G., Allen, A.P. *et al*. 2014. Methane fluxes show consistent temperature dependence across microbial to ecosystem scales. *Nature*, **507**, 488–491, https://doi.org/10.1038/nature13164

Zieger, J., Rothe, J., Hofmann, M., Gärtner, A. and Linnemann, U. 2019. The Permo-Carboniferous Dwyka Group of the Aranos Basin (Namibia) – how detrital zircons help understanding sedimentary recycling during a major glaciation. *Journal of African Earth Sciences*, **158**, 103555, https://doi.org/10.1016/j.jafrearsci.2019.103555